Electronic Transactions on Numerical Analysis.
Volume 2, pp. 22-43, March 1994.

ISSN 1068-9613.

ETNA
Kent State University
etna@mcs.kent.edu

MULTIGRID CONFORMAL MAPPING VIA THE SZEGŐ KERNEL*

BARRY LEE† AND MANFRED R. TRUMMER‡

Abstract. We introduce a multilevel scheme to solve a second kind integral equation which is important in computing conformal maps. This scheme outperforms conjugate gradient methods previously employed for smooth regions. An analysis of the two-grid scheme is provided.

Key words. conformal mapping, multigrid, Szegő kernel, integral equations.

AMS subject classifications. 45L10, 45B05, 65R20, 65F20, 65F10.

1. Introduction. Conformal mapping has received a lot of attention in the early years of numerical analysis (see [4]). There has been considerably increased interest in the field during the past 15 years, and many new and competitive algorithms have entered the field (see e.g. [11, 5]). A major reason for this is the increased use of numerical grid generators. However, a problem in numerical grid generation is the possible inaccuracy in the created grids, and since the grid is generated through the computed Riemann map, it is a problem of computing the Riemann map accurately. Hence, we have a problem in numerical conformal mapping. One method that has the ability to achieve high accuracy is described in [10, 12]. This mapping is found by solving a second kind Fredholm integral equation whose solution is the Szegő kernel. In the present paper, we extend this research by applying a multigrid method to the discretized integral equation.

The aim of this adaption is to achieve rapid convergence for solving the discretized systems. This may appear rather unnecessary since the generalized conjugate gradient (CG) method of [3, 14] converges at respectable rates for these systems (see [12]). But for large n, i.e. fine discretizations, it is faster to reconstruct the (complex-valued) matrix of the discretized system for each iteration rather than storing it out of core memory. Therefore, each CG iteration requires about $10n^2$ flops. Hence, a modest reduction in the number of fine grid iterations can produce a large reduction in the number of operations.

In fact, it appears intuitively that multigrid is the ideal iteration for solving second kind Fredholm integral equations involving compact operators, as is the case for our equations. Since the eigenvalues of a compact operator converge to zero, it is rather easy to choose a smoother that rapidly eliminates the error components corresponding to these eigenvalues. Also, if the trivial injection operator is used, then these are the components that are poorly approximated by the coarse grid correction. Hence, the poorly approximated frequencies of the coarse grid operation, i.e., frequencies lying near the null space of the residual transfer operator, can be damped off by the fine grid smoother. Moreover, exploiting the smoothness of the kernel, by using the obviously chosen Picard smoother, one sees that the error components corresponding to the large eigenvalues are exactly the frequencies that are poorly eliminated on the fine

* This research was supported by the Natural Sciences and Engineering Research Council of Canada (NSERC) grant OGP0036901, NSERC and Schweizerischer Nationalfonds zur Förderung der Wissenschaften BEF 0150297, and Forschungsinstitut für Mathematik, ETH Zürich. Received December 8, 1993. Accepted for publications March 4, 1994. Communicated by M. Gutknecht.

† Program in Applied Mathematics, Campus Box 526, University of Colorado at Boulder, Boulder, Colorado 80309-0526, U.S.A. (blee@newton.colorado.edu).

‡ Department of Mathematics, Simon Fraser University, Burnaby, British Columbia V5A 1S6, Canada (trummer@sfu.ca).

ETNA
Kent State University
etna@mcs.kent.edu

grid but which can be effectively eliminated on the coarser grids. All the elements of a multigrid method are thus present.

We divide the paper into four sections. In section 2, we give a brief derivation of the integral equation and show how the Szegő kernel is related to the Riemann map. Results here are extracted from [9, 10, 12]. The discretization of the equation and the numerical procedure are given in the next section, and some of the convergence details are given in section 4. The latter includes a derivation of the multigrid iteration matrix, and derives a bound on the norm of this matrix. Finally, section 5 gives some numerical examples.

2. The integral equation. Let Ω be an open, bounded, simply connected domain in the complex plane, and let its boundary $\partial\Omega$ be twice continuously differentiable so that it admits a C^2 parametrization $z(t),\ 0 \le t \le \beta$. Also, denote the unit tangent to $\partial\Omega$ at z by $\dot\gamma(z) = \dot z(t)/\left|\dot z(t)\right|$, and denote the arclength on $\partial\Omega$ by $d\sigma$.

The problem is to construct the Riemann mapping function $R(z)$ such that $R(z)$ maps $\overline{\Omega}$ onto the closed unit disk and satisfies $R(a) = 0,\ R'(a) > 0$ for any fixed $a \in \Omega$ (see e.g. [13] for the extension of the Riemann map to the boundary).

DEFINITION 2.1. *The Cauchy kernel H is defined by*

$$H(w,z) = \frac{1}{2\pi i}\frac{\dot\gamma(z)}{z-w}, \quad w \in \overline{\Omega},\ w \neq z,\ z \in \partial\Omega;$$

the Kerzman-Stein kernel is defined by

$$A(w,z) = \begin{cases} \overline{H}(z,w) - H(w,z) & w,\ z \in \partial\Omega,\ w \neq z \\ 0 & w = z \in \partial\Omega. \end{cases}$$

If we let $\mathcal{H}$ denote the integral operator with kernel H, then $\mathcal{H} : \mathcal{L}^2(\partial\Omega, d\sigma) \to \mathcal{K}^2(\partial\Omega, d\sigma)$, the Hardy space, which is the closed subspace of $\mathcal{L}^2(\partial\Omega, d\sigma)$ consisting of elements that are the boundary value of some holomorphic function in Ω in the $\mathcal{L}^2$ sense. This follows because H is the kernel in the Cauchy integral formula. Note that $\mathcal{H}$ is an oblique projector into $\mathcal{K}^2$, and that H has the reproducing property.

Moreover, if we denote by $\mathcal{A}$ the integral operator with kernel A, then $\mathcal{A} : \mathcal{L}^2 \to \mathcal{L}^2$, and

$$\mathcal{A} = \mathcal{H}^* - \mathcal{H}.$$

$\mathcal{A}$ measures the "amount" by which $\mathcal{H}$ fails to be an orthogonal projector. $\mathcal{A}$ is also a compact operator since A is a continuous function on $\partial\Omega \times \partial\Omega$ as shown in [10, 9], and $\mathcal{A}$ has purely imaginary eigenvalues since A is skew-Hermitian.

Another kernel that has the reproducing property and whose corresponding integral operator is a projection from $\mathcal{L}^2$ into $\mathcal{K}^2$ is the Szegő kernel $S(z,w)$. The corresponding integral operator $\mathcal{S}$ is in fact an orthogonal projection. Furthermore, since the Szegő kernel for the unit disk is known explicitely, it follows by conformal transplantation from Ω to the unit disk that

$$R'(z) = \frac{2\pi}{S(a,a)} S^2(z,a), \quad z \in \overline{\Omega}.$$

An argument in [10] leads then to the simple formula for the Riemann mapping function

$$R(z) = -i\dot\gamma(z)\frac{R'(z)}{|R'(z)|}, \quad z \in \partial\Omega.$$

ETNA
Kent State University
etna@mcs.kent.edu

Hence, to compute the Riemann mapping function, we only need to compute the Szegő kernel. One approach uses the fact that if $\{\theta_j\}$ is an arbitrary complete orthonormal system in $\mathcal{K}^2$ (in the measure $d\sigma$), then

$$S(z,w) = \sum_{j=1}^{\infty} \theta_j(z)\overline{\theta_j}(w), \quad w \in \partial\Omega,\ z \in \Omega.$$

The series is simply truncated. But because the orthonormal functions must be computed, this method is often computationally unstable. A better method uses the fact that S is the solution of an integral equation.

THEOREM 2.2. *$S(z,a)$ is the unique solution of the integral equation*

$$S(z,a) + \int_{w\in\partial\Omega} A(z,w)S(w,a)\,d\sigma_w = \overline{H}(a,z), \quad z \in \partial\Omega. \tag{2.1}$$

(See [10] and [12] for a proof.)

Written in operator notation, (2.1) is

$$(\mathcal{I} + \mathcal{A})\,\mathcal{S} = \mathcal{H}^*, \tag{2.2}$$

which can be seen by noting that $\mathcal{HS} = \mathcal{H}$ and $\mathcal{SH} = \mathcal{S}$ since both operators project onto the same subspace.

The reader is also referred to [8] for an illuminating alternate derivation of the integral equation (2.1).

Often the region of interest possesses some symmetry. In such cases, (2.1) can be transformed into another integral equation as described in [12].

DEFINITION 2.3. *Let Ω be a simply connected domain in $\mathcal{C}$, whose boundary is a closed Jordan curve. A complex-valued function λ that satisfies*

$$z \in \partial\Omega,\ \lambda(z) = \lambda(w) \Longrightarrow w \in \partial\Omega$$

is called a symmetry identification function of Ω.

Domains that are invariant under rotations about the origin with angle $2\pi/j$ are of special interest. The identification function here is $\lambda(z) = z^j$, and using a geometric argument we have

$$\lambda(z) = \lambda(w) \qquad \Longrightarrow \qquad S(z,0) = S(w,0). \tag{2.3}$$

Now, with the notation

$$(\partial\Omega)_j := \partial\Omega \bigcap \{z : 0 \le \arg z \le 2\pi/j\},$$

equation (2.1) can be transformed into

$$S(z,0) + \int_{w\in(\partial\Omega)_j} A_S(z,w)S(w,0)\,d\sigma_w = \overline{H}(0,z), \quad z \in (\partial\Omega)_j, \tag{2.4}$$

where

$$\begin{aligned} A_S(z,w) &:= \sum_{\lambda(v)=\lambda(w),\ v\in\partial\Omega} A(z,v) \\ &= \begin{cases} \overline{H_S(w,z)} - H_S(z,w), & w,z \in (\partial\Omega)_j,\ w \ne z, \\ \frac{(1-j)}{2\pi i} Re\left(\frac{\dot\gamma(z)}{z}\right), & w = z \in (\partial\Omega)_j, \end{cases} \end{aligned}$$

ETNA
Kent State University
etna@mcs.kent.edu

$$\begin{aligned} H_S(z,w) &:= \sum_{\lambda(v)=\lambda(w),\ v\in\partial\Omega} H(z,v) \\ &= \frac{1}{2\pi i}\frac{\lambda'(w)\dot\gamma(w)}{\lambda(w)-\lambda(z)}, \quad w\in\overline{\Omega},\ z\in(\partial\Omega)_j,\ \lambda(z)\neq\lambda(w). \end{aligned}$$

THEOREM 2.4. *For a domain Ω that is invariant under rotations about the origin with angle $2\pi/j$ the Szegő kernel function $S(z,0)$, $z\in\partial\Omega$, is the solution of the integral equation (2.4). The values of $S(z,0)$ for $z\notin(\partial\Omega)_j$ can be reconstructed from equation (2.3). Moreover, the operator corresponding to the kernel $A_S(z,w)$ is compact in $C\left((\partial\Omega)_j\right)$.*

Proof. The proof is similar to the one given in [9] for $j=1$. We will assume that the derivative of $\ddot\gamma(s)$ is bounded, although not necessarily continuous.

Clearly, $A_S(z,w)$ is continuous for $z\neq w$ since A_S is restricted to $(\partial\Omega)_j\times(\partial\Omega)_j$; that is, $\lambda(z)=\lambda(w)$ if and only if $z=w$. For $z\approx w$, say $z=\gamma(s),\ w=\gamma(t),\ s\approx t$. We have

$$z(s)=\gamma(s)=\gamma(t)+\dot\gamma(t)(s-t)+\ddot\gamma(t)(s-t)^2+(s-t)^3 r$$

$$w(t)=\gamma(t),$$

where r denotes a generic remainder function factor. Hence,

$$\begin{aligned} \lambda(z) &= \left[\gamma(t)+\dot\gamma(t)(s-t)+\ddot\gamma(t)(s-t)^2+(s-t)^3 r\right]^j \\ &= \gamma^j(t)+j\gamma^{j-1}(t)\dot\gamma(t)(s-t)+\frac{j}{2}\left[\ddot\gamma(t)\gamma^{j-1}(t)+(j-1)\gamma^{j-2}(t)\dot\gamma^2(t)\right] \\ &\qquad (s-t)^2+(s-t)^3 r, \end{aligned}$$

$$\begin{aligned} \lambda(z)-\lambda(w) &= j\gamma^{j-1}(t)\dot\gamma(t)(s-t)+\frac{j}{2}\left[\ddot\gamma(t)\gamma^{j-1}(t)+(j-1)\gamma^{j-2}(t)\dot\gamma^2(t)\right] \\ &\qquad (s-t)^2+(s-t)^3 r \\ &= j\gamma^{j-1}(t)\dot\gamma(t)(s-t)\left[1+\frac{1}{2}\frac{\ddot\gamma(t)}{\dot\gamma(t)}(s-t)+\frac{j-1}{2}\frac{\dot\gamma(t)}{\gamma(t)}(s-t)\right. \\ &\qquad \left.+(s-t)^2 r\right], \end{aligned}$$

and

$$\begin{aligned} \frac{1}{\lambda(z)-\lambda(w)} &= \frac{1}{j\gamma^{j-1}(t)\dot\gamma(t)(s-t)}\left[1-\tfrac{1}{2}\tfrac{\ddot\gamma(t)}{\dot\gamma(t)}(s-t)\right. \\ &\qquad \left.-\tfrac{j-1}{2}\tfrac{\dot\gamma(t)}{\gamma(t)}(s-t)+(s-t)^2 r\right]. \end{aligned} \tag{2.5}$$

ETNA
Kent State University
etna@mcs.kent.edu

Also,

$$\begin{aligned}\lambda'(z)\dot\gamma(z) &= \Big\{j\gamma^{j-1}(t)+j(j-1)\gamma^{j-2}(t)\dot\gamma(t)(s-t)+\Big[\tfrac{j(j-1)}{2}\gamma^{j-2}(t)\ddot\gamma(t)\\ &\qquad +\tfrac{j(j-1)(j-2)}{2}\gamma^{j-3}(t)\dot\gamma^2(t)\Big](s-t)^2+(s-t)^3r\Big\}\\ &\qquad \times\left\{\dot\gamma(t)+\ddot\gamma(t)(s-t)+(s-t)^2r\right\} \qquad (2.6)\\ &= j\dot\gamma(t)\gamma^{j-1}(t)+j\ddot\gamma(t)\gamma^{j-1}(t)(s-t)+j(j-1)\gamma^{j-2}(t)\dot\gamma^2(t)(s-t)\\ &\qquad +(s-t)^2r.\end{aligned}$$

Multiplying (2.5) and (2.6), we have

$$\begin{aligned}2\pi i H_S(w,z) &= \tfrac{\lambda'(z)\dot\gamma(z)}{\lambda(z)-\lambda(w)}\\ &= \tfrac{1}{s-t}+\tfrac{1}{2}\tfrac{\ddot\gamma(t)}{\dot\gamma(t)}+\tfrac{j-1}{2}\tfrac{\dot\gamma(t)}{\gamma(t)}+(s-t)r.\end{aligned} \qquad (2.7)$$

A similar procedure gives

$$\begin{aligned}\tfrac{\lambda'(w)\dot\gamma(w)}{\lambda(w)-\lambda(z)} &= -\tfrac{\lambda'(w)\dot\gamma(w)}{\lambda(z)-\lambda(w)}\\ &= -\left[\tfrac{1}{s-t}-\tfrac{1}{2}\tfrac{\ddot\gamma(t)}{\dot\gamma(t)}-\tfrac{j-1}{2}\tfrac{\dot\gamma(t)}{\gamma(t)}+(s-t)r\right].\end{aligned} \qquad (2.8)$$

So, since $s,t\in\Re$ and $\ddot\gamma(t)\perp\dot\gamma(t)$,

$$\begin{aligned}A_S(w,z) &= \overline{H_S(z,w)}-H_S(w,z), \qquad z\approx w\\ &= \frac{1}{2\pi i}\left\{-Re\left(\frac{\ddot\gamma(t)}{\dot\gamma(t)}\right)+(1-j)Re\left(\frac{\dot\gamma(t)}{\gamma(t)}\right)+(s-t)r\right\}\\ &= \frac{1}{2\pi i}(1-j)Re\left(\frac{\dot\gamma(t)}{\gamma(t)}\right)+(s-t)r;\end{aligned}$$

that is, $A_S(w,z)$ is continuous on $(\partial\Omega)_j\times(\partial\Omega)_j$. □

One can take advantage of additional symmetries (e.g., under reflections about the real or imaginary axes, see [12]). Although the numerical examples will exploit any symmetry, we will consider equation (2.1) for the remainder of this paper unless otherwise specified.

3. Description of the method. To preserve the skew-Hermitian property of the kernel when an arbitrary parametrization of $\partial\Omega$ is used, equation (2.1) is written in the form

$$\eta(t)+\int_0^\beta k(t,s)\eta(s)\,ds=\phi(t),\quad 0\le t\le\beta, \qquad (3.1)$$

where

$$\begin{aligned}\eta(t) &:= |\dot z(t)|^{\frac12}S\left(z(t),a\right),\\ \phi(t) &:= |\dot z(t)|^{\frac12}\overline{H\left(a,z(t)\right)},\ \text{and}\\ k(t,s) &:= |\dot z(t)|^{\frac12}A\left(z(t),z(s)\right)|\dot z(s)|^{\frac12}\end{aligned}$$

(see [10, 12]). Applying Nyström's method with an n-point trapezoid rule to (3.1), which is numerically equivalent to a Fourier-Galerkin method (see [2]), we have the

ETNA
Kent State University
etna@mcs.kent.edu

discrete system

$$\eta\left(t_i^h\right) + h\sum_{j=1}^{n} K^{hh}\left(t_i^h, t_j^h\right)\eta\left(t_j^h\right) = \phi\left(t_i^h\right), \quad 1 \le i \le n, \tag{3.2}$$
$$h = \frac{\beta}{n}, \quad t_i^h = (i-1)h.$$

Or, letting

$$\begin{aligned} B^{hh} &= \left[hK^{hh}\left(t_i^h, t_j^h\right)\right]_{i,j=1}^{n}, \\ \underline{x}_h &= \left[\eta\left(t_i^h\right)\right]_{i=1}^{n}, \\ \underline{y}_h &= \left[\phi\left(t_i^h\right)\right]_{i=1}^{n}, \end{aligned}$$

we obtain the system

$$(I + B^{hh})\underline{x} = \underline{y}. \tag{3.3}$$

In [12] the generalized conjugate gradient method was used to solve this system. It was shown there that the spectrum of the matrix $I + B^{hh}$ is contained in the set $\{\lambda : |Im\ \lambda| \le \beta \max_{t,s} |k(t,s)|,\ Re\ \lambda = 1\}$. But by taking advantage of both the smoothness of $k(t,s)$, which is dictated by the smoothness of $\partial\Omega$ (see [10]), and the high accuracy of the trapezoid rule for periodic functions, the second kind multigrid methods of Hackbusch [6, 7] may be more effective.

The algorithm for a basic second kind multigrid is

Algorithm $\mathbf{MG}_1^h\left(\underline{x}_h, \underline{y}_h\right)$

(i) relax once on $(I^{hh} + B^{hh})\underline{x}_h = \underline{y}_h$ with the initial approximation $\underline{x}_h$ using the Picard smoother;

(ii) if $h = h_{\max}$, then solve the coarse grid exactly or iteratively; otherwise,
  a. restrict the defect: $d_{2h} = {I_h}^{2h}\left(\underline{x}_h + B^{hh}\underline{x}_h - \underline{y}_h\right)$
  b. $\underline{u}_{2h} = 0$
  c. $\underline{u}_{2h} \longleftarrow \mathbf{MG}_1^{2h}\left(\underline{u}_{2h}, \underline{d}_{2h}\right)$ twice;

(iii) interpolate the coarse grid correction:

$$\underline{x}_h \longleftarrow \underline{x}_h - {I_{2h}}^h\underline{u}_{2h}.$$

By noting that no matrix multiplication is required whenever the initial approximation is zero, and that the trivial injection permits the defect to be calculated in only 0.5 matrix multiplications on the standing grid, one can obtain a good estimate of the work done per iteration: Let there be l levels with the coarsest level numbered zero. The number of visits to each level is

$$2^{l-k} \text{ on level } k, \quad 1 \le k \le l.$$

On level k, the number of fine grid WU's — i.e., the cost of one fine grid matrix-vector multiplication — is

$$\left[2^{-(l-k)}\right]^2.$$

ETNA
Kent State University
etna@mcs.kent.edu

Now each visit requires a defect calculation. Hence,

$$\frac{1}{2}\left[1+2^{-1}+2^{-2}+\cdots+2^{-l+1}\right]\ \text{WU}'\text{s} = (1-2^{-l})\ \text{WU}'\text{s}$$

are required for all the defects. Also, for each 2 visits to level k, $1 \le k \le l-1$, only one matrix-vector multiplication is performed. Hence, omitting the costs of the coarsest grid calculations, there are 2^{l-k-1} "active" visits to level k, and the total number of operations required for the smoothing is

$$\left[1+2^{-2}+2^{-3}+\cdots+2^{-l}\right]\ \text{WU}'\text{s} = \left\{2\left[1-2^{-l-1}\right]-\frac{1}{2}\right\}\ \text{WU}'\text{s}.$$

The total cost is then

$$(1-2^{-l})+2(1-2^{-l-1})-\frac{1}{2} \approx 2\frac{1}{2}\ \text{WU}'\text{s}.$$

Thus, each multigrid iteration is equivalent to 2.5 Picard or conjugate gradient iterations.

Further reduction is possible if in (ii)c., instead of calling $\mathbf{MG}_1^{2h}\left(\underline{u}_{2h}, \underline{d}_{2h}\right)$ twice with the effect that two Picard relaxations are performed on the standing grid, we can relax only at the second call. This modification does not only exploit the smoothness of the defect, but it also has better convergence properties when $\left\|B^{hh}\right\| \gg 1$. We examine this in the next section. The work load drops down to ≈ 2.25 WU's because each 2 visits will now require only one defect calculation.

Another modification to the algorithm is to apply nested iteration using the Nyström interpolant

$$\underline{x}_{h,i} = \begin{cases} \underline{x}_{2h,i} & \text{if the } i'\text{th node is common} \\ \underline{y}_{h,i} - \sum_{j=1}^{\frac{n}{2}} 2hB_{ij}^{h,2h}\underline{x}_{2h,j} & \text{otherwise.} \end{cases}$$

This is of course an expensive interpolation formula, but this interpolation permits us to omit the first smoothing on the interpolated level. With this omission, the work load is approximately $\frac{7}{3}$ WU's.

4. Convergence of the scheme. To see how the coarse grid correction acts on the eigenvalues of the integral operator $\mathcal{K}$ corresponding to the kernel $k(t,s)$, first note that the two grid matrix for the modified w-cycle is

$$\begin{aligned} M_h^{TGM} &:= \left[I^{hh} - I_{2h}{}^h\left(I^{2h,2h}+B^{2h,2h}\right)^{-1} I_h{}^{2h}\left(I^{hh}+B^{hh}\right)\right]\left(-B^{hh}\right) \\ &= A_h^{TGM}\left(-B^{hh}\right), \end{aligned}$$

where A_h^{TGM} is the bracketed factor. Second, recall that the compactness of $\mathcal{K}$ guarantees that its eigenvalues $\lambda_j \to 0$, although the sequence may oscillate to this limit from above and below the real axis (purely imaginary eigenvalues). One asymptotic estimate of this rate of convergence can be obtained by observing that $|\lambda_j| = |\sigma_j|$, the j'th singular value of $\mathcal{K}$, and if $k(t,s)$ is assumed to be continuously differentiable on $(0,\beta)$, then

$$|\sigma_j| = O\left(j^{-\frac{3}{2}}\right).$$

ETNA
Kent State University
etna@mcs.kent.edu

The obvious problem is that the smaller eigenvalues will be poorly approximated when $\mathcal{K}$ is discretized. Not only may B^{hh} have a non-trivial null space, but also the smaller eigenvalues may have the opposite signs of the exact eigenvalues. Mathematically these two problems can be illustrated by using the facts that $\left\{B^{hh}\right\}_h$ is collectively compact, $B^{hh} \to \mathcal{K}$, and hence $\left\{B^{hh} - \mathcal{K}\right\}$ is collectively compact (see [1]). For every open set $\Gamma \supset \sigma(\mathcal{K})$ then, there exists an N such that $\Gamma \supset \sigma\left(B^{hh}\right),\ n \geq N$. In particular, if we let

$$\Gamma_\epsilon(K) = \bigcup_{\lambda \in \sigma(\mathcal{K})} \Gamma_\epsilon(\lambda), \quad \Gamma_\epsilon(\lambda) = \{z : |z - \lambda| \leq \epsilon\},$$

then there exists some N_ϵ such that

$$\Gamma\left(B^{hh}\right) \subset \Gamma_\epsilon(K) \quad n \geq N_\epsilon.$$

Taking $\lambda = 0$, the disc Γ_0 will contain an infinite number of spectral values, and the smaller eigenvalues of B^{hh} will be contained in this disc for sufficiently small h.

But note that these problems are inevitable. The equation must be discretized, and so the only thing we can expect is that the poor approximations do not affect the convergence of the iterative scheme (i.e., convergence independent of discretization). On the other hand, since the trapezoid rule applied to a periodic kernel and a periodic forcing term is equivalent to the Fourier Galerkin method, the large eigenvalues are accurately approximated. This may be exploited.

We are ready to examine the damping effect of the two-grid scheme. Since the smoothing rapidly eliminates the high frequencies ($B^{hh}\underline{v_i^h} = \lambda_i \underline{v_i^h}$), the coarse grid correction must reduce the smooth frequencies, or the eigenvectors corresponding to the large eigenvalues. Now using the injection operator, the transfer residual operator ${I_h}^{2h}\left(I^{hh} + B^{hh}\right)$ simply involves the odd rows of $\left(I^{hh} + B^{hh}\right)$. This reduced matrix has a null space of dimension of at least $\frac{(n-1)}{2}$,[1] and it is also an approximation of $(\mathcal{I} + \mathcal{K})$. Hence, the null space of the residual transfer operator will be approximately in the span of the high frequencies. The smooth frequencies, moreover, which are well approximated by the trapezoid method even on the coarse grid can then be eliminated on the coarse grid. Using a piecewise polynomial interpolant, the interpolation operator ${I_{2h}}^h$ has full rank. And because the residual equation is a discrete approximation of

$$(\mathcal{I} + \mathcal{K})\, e = (\mathcal{I} + \mathcal{K})\, x - y = r,$$

the continuity (smoothness) of the forcing term guarantees the continuity (smoothness) of e. This guarantees a good damping of the smooth frequencies by the coarse grid correction.

To obtain a bound on M_h^{TGM}, we introduce the spaces $\mathcal{U}$ and $\mathcal{V}$. The integral operator $\mathcal{K}$ maps $\mathcal{U}$ into $\mathcal{V}$, which is "more smooth". Since the forcing term

$$\overline{H(a,z)} = \overline{\frac{1}{2\pi i}\frac{\dot\gamma(z)}{z-a}}$$

is continuous of order $\mathcal{C}^{j-1}(\partial\Omega)$ if $a \notin \partial\Omega$ and $\partial\Omega$ is of order $\mathcal{C}^j$, and since A is of order $\mathcal{C}^{j-2}(\partial\Omega \times \partial\Omega)$ under the same conditions on $\partial\Omega$, $\mathcal{U}$ is of order $\mathcal{C}^{j-2}(\partial\Omega)$.[2]

[1] We will assume that n is odd.
[2] If the kernel $k(t,s) \in \mathcal{C}^{j-1}(\partial\Omega \times \partial\Omega)$ and $y(t) \in \mathcal{C}^{j-1}(\partial\Omega)$, then $x(t) \in \mathcal{C}^{j-1}(\partial\Omega)$.

ETNA
Kent State University
etna@mcs.kent.edu

Note that using the norm

$$\|u\|_{\mathcal{C}^m(\partial\Omega)} = \max_{0\le\alpha\le m} \|D^\alpha u\|_\infty \quad m = j-1,\ j-2,$$

where D^α is the derivative operator of order α, $\mathcal{K}$ is a compact operator in $\mathcal{C}^{j-2}(\partial\Omega)$. This follows because weak convergence in $\mathcal{C}^{j-2}(\partial\Omega)$ implies weak convergence in $\mathcal{C}^0(\partial\Omega)$, and because the kernel is order $\mathcal{C}^{j-2}(\partial\Omega\times\partial\Omega)$; that is, because of the compactness of $D^\alpha A$ in $\mathcal{C}^0(\partial\Omega)$.

Also, introduce the discrete analogues of the spaces $\mathcal{U}$ and $\mathcal{V}$, denoted by U, V. The discrete norms will be

$$\|\underline{u}\|_U = \max_{0\le\alpha\le m} \|\underline{D}^\alpha \underline{u}\|_\infty ,$$

where $\underline{D}^\alpha$ is the discrete derivative operator of order α. In the remainder of the paper, we will take $\mathcal{U} = \mathcal{V} = \mathcal{L}^2(\partial\Omega)$ and omit the subscripting of the norm.

Now a bound for the two grid matrix is

$$\begin{aligned}
\left\|M_h^{TGM}\right\| &= \left\|\left[I^{hh} - {I_{2h}}^h \left(I^{2h,2h} + B^{2h,2h}\right)^{-1} {I_h}^{2h} \left(I^{hh} + B^{hh}\right)\right] B^{hh}\right\| \\
&= \left\|\left\{I^{hh} - {I_{2h}}^h {I_h}^{2h} + {I_{2h}}^h \left(I^{2h,2h} + B^{2h,2h}\right)^{-1}\right.\right. \\
&\qquad \left.\left.\left[\left(I^{2h,2h} + B^{2h,2h}\right) {I_h}^{2h} - {I_h}^{2h}\left(I^{hh} + B^{hh}\right)\right]\right\} B^{hh}\right\| \\
&\le \left[\left\|I^{hh} - {I_{2h}}^h {I_h}^{2h}\right\| + \left\|{I_{2h}}^h\right\| \left\|\left(I^{2h,2h} + B^{2h,2h}\right)^{-1}\right\|\right. \\
&\qquad \left.\left\|B^{2h,2h} {I_h}^{2h} - {I_h}^{2h} B^{hh}\right\|\right] \left\|B^{hh}\right\|
\end{aligned}$$

An application of the Gerschgorin theorem shows that

$$\left\|B^{hh}\right\|_\infty \le \beta \max_{t,s} |k(t,s)| =: C_{\infty k}, \tag{4.1}$$

which may be used to approximate

$$C_B := \left\|B^{hh}\right\|; \tag{4.2}$$

because $B^{2h,2h}$ is skew-Hermitian,

$$\left\|\left(I^{2h,2h} + B^{2h,2h}\right)^{-1}\right\| \le 1. \tag{4.3}$$

As for the term

$$\left\|I - {I_{2h}}^h {I_h}^{2h}\right\|,$$

if ${I_h}^{2h}$ is the injection operator and ${I_{2h}}^h$ is a piecewise polynomial interpolation operator of degree $r, r \le j-2$, then

$$\begin{aligned}
\left\|I - {I_{2h}}^h {I_h}^{2h}\right\| &= O\left(h^{r+1}\right) \\
&= C_I h^{r+1};
\end{aligned} \tag{4.4}$$

ETNA
Kent State University
etna@mcs.kent.edu

and for the term

$$\left\| {I_{2h}}^{h} \right\| =: C_p,$$

C_p is usually about one. The remaining factor reflects the smoothness of the kernel. To obtain a computable bound on this term, let $u \in C^{j-2}(\partial\Omega)$ and let $\underline{u_l}$ be its grid function approximant. Note that with the trivial injection,

$$ {I_h}^{2h} B^l \underline{u_l} = \begin{pmatrix} \sum_{i=1}^{n} B^l_{1i} u_{li} \\ \sum_{i=1}^{n} B^l_{2i} u_{li} \\ \cdot \cdot \cdot \\ \cdot \cdot \cdot \\ \cdot \cdot \cdot \\ \sum_{i=1}^{n} B^l_{ni} u_{li} \end{pmatrix} \in \mathcal{C}^{\frac{n+1}{2}}, $$

$$ B^{l-1} {I_h}^{2h} \underline{u_l} = \begin{pmatrix} \sum_{i=1}^{\frac{n+1}{2}} B^{l-1}_{1i} u_{l,(2i-1)} \\ \sum_{i=1}^{\frac{n+1}{2}} B^{l-1}_{2i} u_{l,(2i-1)} \\ \cdot \cdot \cdot \\ \cdot \cdot \cdot \\ \cdot \cdot \cdot \\ \sum_{i=1}^{\frac{n+1}{2}} B^{l-1}_{\frac{n+1}{2},i} u_{l,(2i-1)} \end{pmatrix} = \begin{pmatrix} \sum_{i=1}^{\frac{n+1}{2}} 2B^l_{1,2i-1} u_{l,(2i-1)} \\ \sum_{i=1}^{\frac{n+1}{2}} 2B^l_{3,2i-1} u_{l,(2i-1)} \\ \cdot \cdot \cdot \\ \cdot \cdot \cdot \\ \cdot \cdot \cdot \\ \sum_{i=1}^{\frac{n+1}{2}} 2B^l_{n,2i-1} u_{l,(2i-1)} \end{pmatrix} \in \mathcal{C}^{\frac{n+1}{2}}. $$

Taking a random row (actually we can take the row corresponding to the infinity norm for $l = 0$), say row p, then

$$\begin{aligned} C_{rB} &:= \left\| B^{l-1} {I_h}^{2h} - {I_h}^{2h} B^l \right\| \\ &\approx \left\| B^{l-1} {I_h}^{2h} - {I_h}^{2h} B^l \right\|_\infty \\ &\approx \left| 2 \sum_{i=1}^{\frac{n+1}{2}} B^l_{p,2i-1} u_{l,2i-1} - \sum_{i=1}^{n} B_{p,i} u_{l,i} \right| \\ &= \left| \sum_{i=1}^{\frac{n+1}{2}} B^l_{p,2i-1} u_{l,2i-1} - \sum_{i=1}^{\frac{n-1}{2}} B^l_{p,2i} u_{l,2i} \right|. \end{aligned}$$

Since $u \in C^{j-2}(\partial\Omega)$, if a sufficient number of nodes are used, $u_{l,2i-1} \approx u_{l,2i}$. Hence,

$$\left\| B^{l-1} {I_h}^{2h} - {I_h}^{2h} B^l \right\|_\infty \approx \left| \sum_{i=1}^{\frac{n-1}{2}} \left(B^l_{p,2i-1} - B^l_{p,2i} \right) \right|,$$

which is small if $k(t,s)$ is very smooth in t, and which may be used to approximate C_{rB}.

An a priori estimate is also available. Using the periodicity of $k(t,s)$ and $u(s)$, we have

ETNA
Kent State University
etna@mcs.kent.edu

$$\begin{aligned}
\left\| B^{l-1} {I_h}^{2h} \underline{u}_l - {I_h}^{2h} B^l \underline{u}_l \right\|_\infty &\approx \left| \left(\int_a^b k\left((p-1)h, s\right) u(s)\, ds + error_{trap1} \right) \right. \\
&\quad \left. - \left(\int_a^b k\left((p-1)h, s\right) u(s)\, ds + error_{trap2} \right) \right| \\
&= \left| g_s^{2i-1}(\beta) - g_s^{2i-1}(0) \right| \left| C_{trap1} - 2^{2i} C_{trap2} \right| h^{2i} \\
&\quad + O\left(h^{2i+1}\right) \\
&\approx C'_{rB} h^{2i},
\end{aligned}$$

where i is the maximum integer such that

$$g_s^{2i-3}(\beta) - g_s^{2i-3}(0) = 0,$$

$$g_s = \frac{d}{ds}\left(k\left((p-1)h, s\right) u(s)\right).$$

All of the bounds give

$$\left\| M_l^{TGM} \right\| \leq \left(C_I h^{r+1} + C_p C'_{rB} h^{2i} \right) C_B. \tag{4.5}$$

Remark: Suppose that on a two grid scheme, the defect equation is solved iteratively. Then a non-stationary two grid matrix can be produced:

$$M_{h,i}^{TGM} = \left[I^h - s_i {I_{2h}}^h {I_h}^{2h} + s_i {I_{2h}}^h \left(I^{2h} + B^{2h} \right)^{-1} {I_h}^{2h} \left(I^h + B^h \right) \right] (-B^h),$$

where s_i is a steplength parameter for the i'th iteration. A convenient way of choosing this parameter is to view the defect equation as a minimization of

$$\psi\left(\underline{v}^{2h}\right) = \frac{1}{2} < \left(I^{2h} - B^{2h} B^{2h} \right) \underline{v}^{2h}, \underline{v}^{2h} > - < \left(I^{2h} - B^{2h} \right) \underline{d}^{2h}, \underline{v}^{2h} >$$

over $\mathcal{C}^{\frac{n+1}{2}}$. After p iterations on the coarse grid, we can take the resulting approximation $\underline{v}^{2h^*}$ to be a search direction, and minimize ψ along this direction. In this case,

$$\begin{aligned}
s_i &= \frac{< \left(I^{2h} - B^{2h} \right) \underline{d}^{2h}, \underline{v}^{2h^*} >}{< \left(I^{2h} - B^{2h} B^{2h} \right) \underline{v}^{2h^*}, \underline{v}^{2h^*} >} \\
&= \frac{< \underline{d}^{2h}, \left(I^{2h} + B^{2h} \right) \underline{v}^{2h^*} >}{< \left(I^{2h} + B^{2h} \right) \underline{v}^{2h^*}, \left(I^{2h} + B^{2h} \right) \underline{v}^{2h^*} >}.
\end{aligned}$$

The cost of computing this parameter is then about 0.25 WU's.

This strategy also can be applied throughout the multigrid w-cycle. In this case, since for each visit to level k a prolongation must be computed, there are $2^{l-k}, 1 \leq k \leq l$, steplength parameters to be formed on this level. Each of these parameters requires $\left[2^{-(l+k+1)}\right]^2$ WU's to form. Hence, omitting the cost of the level $k = 1$, which is free if an exact solver is used on the coarsest grid, the total cost is

$$2^{-2}\left[1 + 2^{-1} + \cdots + 2^{-l+2}\right] \text{ WU's} \approx \frac{1}{2} \text{ WU's}.$$

ETNA
Kent State University
etna@mcs.kent.edu

Turning to the full modified w-cycle, the iteration matrix is

$$\begin{aligned} M^l &= \Big[I^l - {I_{l-1}}^l \left(I^{l-1} + A^{l-1}B^{l-1}A^{l-1}\right)\left(I^{l-1} + B^{l-1}\right)^{-1} \\ &\qquad {I_l}^{l-1}\left(I^l + B^l\right)\Big](-B^l) \quad l \geq 1, \end{aligned}$$

where A^{l-1} is defined recursively by

$$\begin{aligned} A^{l-1} &= \Big[I^{l-1} - {I_{l-2}}^{l-1}\left(I^{l-2} + A^{l-2}B^{l-2}A^{l-2}\right)\left(I^{l-2} + B^{l-2}\right)^{-1} \\ &\qquad {I_{l-1}}^{l-2}\left(I^{l-1} + B^{l-1}\right)\Big] \end{aligned}$$

with $A^0 = 0$.

Proof. First, multigrid has the form

$$\underline{x}_l^j = M^l \underline{x}_l^{j-1} + N^l \underline{f}_l. \tag{4.6}$$

Assuming that the iteration matrix is given by the above formula, by following the algorithm, one can see that

$$N^l = I^l + {I_{l-1}}^l \left(I^{l-1} + A^{l-1}B^{l-1}A^{l-1}\right)\left(I^{l-1} + B^{l-1}\right)^{-1} {I_l}^{l-1}(-B^l)$$

if smoothing is performed, and

$$N^l = {I_{l-1}}^l \left(I^{l-1} + A^{l-1}B^{l-1}A^{l-1}\right)\left(I^{l-1} + B^{l-1}\right)^{-1} {I_l}^{l-1}$$

if no smoothing is performed. Now the solution of the discretized system is a fixed point of the Picard smoother:

$$\underline{x}_l = -B^l \underline{x}_l + \underline{f}_l.$$

Replacing M^l and N^l with the above expressions, it can be shown easily that $\underline{x}_l$ is also a fixed point of the multigrid scheme.

It is clear that the formula holds for $l = 1$. Let it also hold for $l - 1$. Then for l, the iteration matrix is of the form

$$C^l B^l,$$

where C^l is the coarse grid correction operator. For simplicity, take $\underline{f}_l$ to be zero. In this case, we have

$$\underline{d}_{l-1} = {I_l}^{l-1}\left(I^l + B^l\right)\underline{\hat{x}}_l,$$

and

$$\underline{u}_{l-1}^j = M^{l-1}\underline{u}_{l-1}^{j-1} + N^{l-1}\underline{d}_{l-1}. \tag{4.7}$$

Now when smoothing is performed,

$$\begin{aligned} N^{l-1} &= I^{l-1} - {I_{l-2}}^{l-1}\left(I^{l-2} + A^{l-2}B^{l-2}A^{l-2}\right)\left(I^{l-2} + B^{l-2}\right)^{-1} {I_{l-1}}^{l-2}B^{l-1} \\ &= I^{l-1} - {I_{l-2}}^{l-1}\left(I^{l-2} + A^{l-2}B^{l-2}A^{l-2}\right)\left(I^{l-2} + B^{l-2}\right)^{-1} \times \end{aligned}$$

ETNA
Kent State University
etna@mcs.kent.edu

$$
\begin{aligned}
& {I_{l-1}}^{l-2}\left(I^{l-1}+B^{l-1}\right)B^{l-1}\left(I^{l-1}+B^{l-1}\right)^{-1} \\
= \quad & \Big[I^{l-1}+B^{l-1}-{I_{l-2}}^{l-1}\left(I^{l-2}+A^{l-2}B^{l-2}A^{l-2}\right)\left(I^{l-2}+B^{l-2}\right)^{-1} \\
& \qquad {I_{l-1}}^{l-2}\left(I^{l-1}+B^{l-1}\right)B^{l-1}\Big]\left(I^{l-1}+B^{l-1}\right)^{-1} \\
= \quad & \left(I^{l-1}-M^{l-1}\right)\left(I^{l-1}+B^{l-1}\right)^{-1};
\end{aligned}
$$

and when no smoothing is performed,

$$
\begin{aligned}
N^{l-1} &= {I_{l-2}}^{l-1}\left(I^{l-2}+A^{l-2}B^{l-2}A^{l-2}\right)\left(I^{l-2}+B^{l-2}\right)^{-1}{I_{l-1}}^{l-2} \\
&= {I_{l-2}}^{l-1}\left(I^{l-2}+A^{l-2}B^{l-2}A^{l-2}\right)\left(I^{l-2}+B^{l-2}\right)^{-1}{I_{l-1}}^{l-2} \\
&\qquad \left(I^{l-1}+B^{l-1}\right)\left(I^{l-1}+B^{l-1}\right)^{-1} \\
&= \left(I^{l-1}+B^{l-1}\right)^{-1}-\Big[I^{l-1}-{I_{l-2}}^{l-1}\left(I^{l-2}+A^{l-2}B^{l-2}A^{l-2}\right) \\
&\qquad \left(I^{l-2}+B^{l-2}\right)^{-1}{I_{l-1}}^{l-2}\left(I^{l-1}+B^{l-1}\right)\Big]\left(I^{l-1}+B^{l-1}\right)^{-1} \\
&= \left(I^{l-1}-A^{l-1}\right)\left(I^{l-1}+B^{l-1}\right)^{-1}.
\end{aligned}
$$

Because we omit smoothing first, and then smooth at the second call, using the initial approximation $\underline{u}_{l-1}^{0}=0$, (4.7) gives

$$
\begin{aligned}
\underline{u}_{l-1}^{2} &= -A^{l-1}B^{l-1}\left(I^{l-1}-A^{l-1}\right)\left(I^{l-1}+B^{l-1}\right)^{-1}\underline{d}_{l-1}+\left(I^{l-1}+A^{l-1}B^{l-1}\right) \\
&\qquad \left(I^{l-1}+B^{l-1}\right)^{-1}\underline{d}_{l-1} \\
&= \left(I^{l-1}+A^{l-1}B^{l-1}A^{l-1}\right)\left(I^{l-1}+B^{l-1}\right)^{-1}{I_{l}}^{l-1}\left(I^{l}+B^{l}\right)\underline{\hat{x}}_{l}.
\end{aligned}
$$

Interpolating this defect solution, we have

$$
\begin{aligned}
C^{l}B^{l}\underline{\tilde{x}}_{l} &= -B^{l}\underline{\tilde{x}}_{l}-{I_{l-1}}^{l}\underline{u}_{l-1}^{2}, \\
&= -\Big[I^{l}-{I_{l}}^{l-1}\left(I^{l-1}+A^{l-1}B^{l-1}A^{l-1}\right)\left(I^{l-1}+B^{l-1}\right)^{-1} \\
&\qquad {I_{l}}^{l-1}\left(I^{l}+B^{l}\right)\Big]B^{l}\underline{\tilde{x}}_{l},
\end{aligned}
$$

where $\underline{\tilde{x}}_{l}$ satisfies

$$\underline{\hat{x}}_{l}=-B^{l}\underline{\tilde{x}}_{l}+\underline{f}_{l}.$$

Hence,

$$C^{l}=-\left[I^{l}-{I_{l}}^{l-1}\left(I^{l-1}+A^{l-1}B^{l-1}A^{l-1}\right)\left(I^{l-1}+B^{l-1}\right)^{-1}{I_{l}}^{l-1}\left(I^{l}+B^{l}\right)\right].$$

As for a bound on this iteration matrix, we have

$$\left\|M^{l}\right\| \quad \leq \quad \left\|A^{l}\right\|\left\|B^{l}\right\|$$

ETNA
Kent State University
etna@mcs.kent.edu

$$\begin{aligned} (4.8) \qquad &= \left\| \left[A_l^{TGM} - {I_l}^{l-1} A^{l-1} B^{l-1} A^{l-1} \left(I^{l-1} + B^{l-1} \right)^{-1} {I_l}^{l-1} \left(I^l + B^l \right) \right] \right\| \left\| B^l \right\| \\ &\leq \left[\left\| A_l^{TGM} \right\| + \left\| {I_l}^{l-1} \right\| \left\| A^{l-1} \right\|^2 \left\| B^{l-1} \right\| \left(C_r + C_s C'_{rB} h_l^{2i} \right) \right] \left\| B^l \right\|. \end{aligned}$$

Since

$$\left\| A^l \right\| \leq \left\| A_l^{TGM} \right\| + C^* \left\| A^{l-1} \right\|^2,$$

where $C^* = O(C_p C_B C_r)$, the recurrence for the upper bound on $\left\| A^l \right\|$ then satisfies

$$\begin{cases} v_1 \leq & v, \\ v_l \leq & v + C^* v_{l-1}^2, \end{cases}$$

where $v := \max_l \left\{ \left\| A_l^{TGM} \right\| \right\}$, or

$$\begin{cases} u_1 \leq & C^* v, \\ u_l \leq & C^* v + u_{l-1}^2, \end{cases} \qquad (4.9)$$

if we let $u_l = C^* v_l$. In the case of equality, (4.9) becomes a nonlinear difference equation. In this situation, consider the polynomial

$$x^2 - x + C^* v.$$

Restricting to only real roots, we must enforce the condition

$$v \leq \frac{1}{4C^*} \qquad (4.10)$$

(we must choose h_1 small enough for this condition to hold!) so that the roots are

$$r_1 = \frac{1}{2} + \frac{\sqrt{1 - 4vC^*}}{2} \qquad \left(\frac{1}{2} \leq r_1 < 1 \right),$$

and

$$r_2 = 1 - r_1 \qquad \left(0 < r_2 \leq \frac{1}{2} \right).$$

Now because the term u_l converges to r_2 if v is sufficiently small,

$$v_l \longrightarrow \frac{r_2}{C^*},$$

and referring to (4.8),

$$\left\| M^l \right\| \longrightarrow \frac{r_2}{C^*} \left\| B^l \right\| = \frac{r_2}{\hat{C}},$$

where $\hat{C} = O(C_p C_r)$. Or, using the restriction on v

$$\begin{cases} u_1 \leq & 0.25, \\ u_l \leq & 0.25 + u_{l-1}^2 \end{cases},$$

we have $u_l \leq 0.5$ for all l. Hence,

$$\left\| M^l \right\| \leq \frac{1}{2\hat{C}} \text{ for all } l.$$

ETNA
Kent State University
etna@mcs.kent.edu

For the strict inequality case, assuming that the sequence converges to say b, then

$$b < C^* v + b^2,$$

implying that $b > r_1$ or $b < r_2$. Again, (4.10) will enforce

$$\left\|M^l\right\| < \frac{1}{2\hat{C}} \text{ for all } l.$$

The above analyses show that

$$\begin{aligned} \left\|M^l\right\| &\leq \left\|M_l^{TGM}\right\| + Dh_l^r \left\|M_l^{TGM}\right\| \\ &= C^{TGM}\left(1 + Dh_l^r\right) h_l^r, \end{aligned}$$

where $Dh_l^r = O(1)$. Hence, the w-cycle is indeed a perturbation of the two-grid scheme. □

Remark 1. The restriction on v is a bit stronger than is needed. Since l is usually of $O(1)$, we can allow v to be larger than $\frac{1}{4C^*}$. But then vice-versa, if v is too large, which occurs if the boundary is not very smooth (i.e., $\left\|B^{l-1}{I_h}^{2h} - {I_h}^{2h}B^l\right\|$ is large), we can expect the multigrid procedure to fare poorly. This in fact was observed in the experiments.

Remark 2. The major cost of a w-cycle is of course the reconstruction of the matrix. It is thus desirable that as few fine grid iterations as possible should be performed. One method that even avoids constructing the finer matrices is to approximate these using sufficiently high degree polynomial interpolants of the coarser matrices. This works well if the kernel or boundary is very smooth. But to show convergence of such a scheme, bounds of the polynomial interpolation operator must be incorporated into the above analyses. Moreover, the accuracy may not be as good as when one reconstructs the matrix because of the "spectral" accuracy of the trapezoid method for our equations.

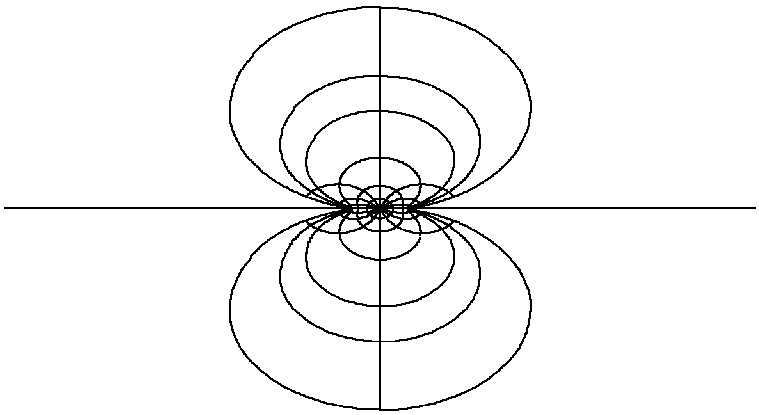

FIG. 5.1. *Inverted ellipse, p= 0.1*

5. Numerical examples. The boundaries that we experimented with are the same as those described in [12]. The experiments were conducted on Sun 4/670 with two processors. As in the paper [12] the boundary correspondence function $\theta(t)$ is computed using the formula

$$\theta(t) = arg\left[-i\eta^2(t)\dot{z}(t)\right],$$

ETNA
Kent State University
etna@mcs.kent.edu

TABLE 5.1
Inverted ellipse, CPU times (in seconds) and errors for multigrid W-cycle and CG algorithm.

	$p = 0.2$		$p = 0.1$		$p = 0.05$	
n	mgw	cg	mgw	cg	mgw	cg
128	0.8	0.8	0.9	0.8	1.1	0.9
	1.06e-4	1.12e-4	8.78e-2	8.81e-2	7.51e-1	7.52e-1
256	2.2	2.5	2.6	2.4	3.8	2.4
	1.87e-7	1.77e-7	4.72e-3	4.31e-3	2.43e-1	2.43e-1
512	7.1	10.3	7.1	9.1	11.0	9.1
	7.37e-11	3.12e-11	2.64e-5	2.14e-5	5.8e-2	5.8e-2
1024	25.9	46.2	26.1	42.3	43.1	38.0
	1.67e-14	4.44e-15	6.73e-8	6.62e-8	3.00e-3	3.01e-3
2048	—	—	104.4	213.8	139.2	180.5
	—	—	5.16e-12	1.95e-11	7.22e-6	7.55e-5
4096	—	—	—	—	558.8	912.8
	—	—	—	—	2.61e-8	2.66e-8

the inverse Riemann mapping function is approximated by an $m-1$ degree trigonometric polynomial using m equally-spaced nodes on the unit circle, and the symmetry of the domain is exploited. The error is taken to be $\|\theta_n - \theta\|_\infty$ (numerically computed by evaluating the difference at $n = 120$ equally-spaced points in the parameter interval of the underlying integral equation).

EXAMPLE 1 (**Inverted Ellipse ($0 < p \leq 1$).**).

$$\begin{aligned} z(t) &= \sqrt{1-(1-p^2)\cos^2 t}\, e^{it}, \\ \tan t &= p\, \tan\theta(t). \end{aligned}$$

Table 5.1 shows the results for the multigrid w-cycle and the generalized conjugate gradient method. For each n, both the cpu time (top value) and the accuracy (bottom value) are given. For the w-cycle, the coarsest grid was chosen such that the coarsest two-grid matrix had an approximate norm of less than .25, and for the conjugate gradient method, we chose the initial approximation to be the forcing term. Both iterations were stopped once the norm of the residual was smaller than the square of the approximate discretization error.

As $p \to 0$, the domain has a sharp "pinch," making the problem harder (see[3] Figure 5.1). We can see that the w-cycle is substantially faster only after enough points are used to decrease the discretization error.

EXAMPLE 2 (**Ellipse ($0 \leq \epsilon < 1$, eccentricity= $\frac{1+\epsilon}{1-\epsilon}$)).**

$$\begin{aligned} z(t) &= e^{it} + \epsilon e^{-it}, \\ \theta(t) &= t + 2\sum_{m=1}^{\infty} \frac{(-1)^m}{m} \frac{\epsilon^m}{1+\epsilon^{2m}} \sin(2mt). \end{aligned}$$

Problems arise once the eccentricity is ≥ 20.0. These values correspond to very thin ellipses.

Figure 5.2 is a logscale graph of the error of the boundary correspondence function for eccentricity= 25.0.

[3] Due to scaling, the contours do not appear to intersect at right angles.

ETNA
Kent State University
etna@mcs.kent.edu

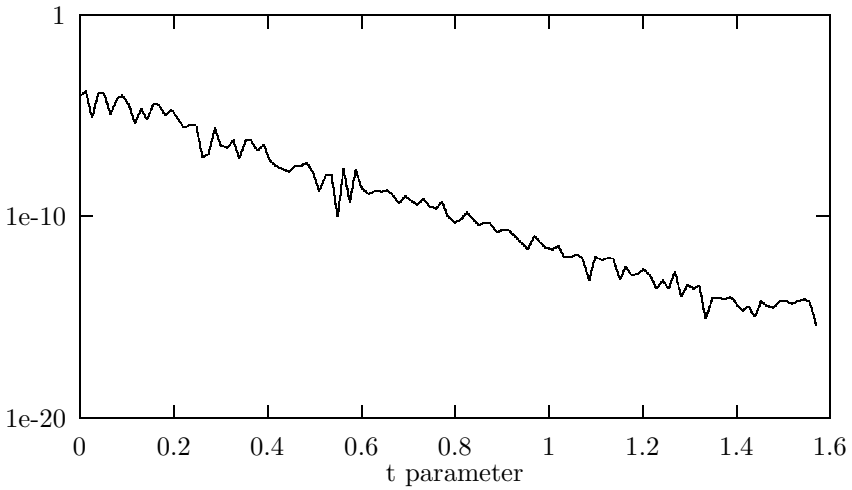

FIG. 5.2. *Boundary correspondence function error for the ellipse, eccentricity= 25.0*

TABLE 5.2
Ellipse, $\hat{\epsilon}$ *= eccentricity=* $\frac{1+\epsilon}{1-\epsilon}$

	$\hat{\epsilon} = 5.0$		$\hat{\epsilon} = 10.0$		$\hat{\epsilon} = 20.0$		$\hat{\epsilon} = 25.0$	
n	mgw	cg	mgw	cg	mgw	cg	mgw	cg
128	.9	1.0	1.2	1.0	—	—	—	—
	1.14e-6	1.12e-6	2.76e0	3.01e0	—	—	—	—
256	3.3	3.7	2.8	3.5	—	—	—	—
	1.89e-11	5.09e-14	7.60e-5	5.46e-4	—	—	—	—
512	—	—	13.8	16.8	9.4	14.9	15.7	22.2
	—	—	4.92e-11	2.26e-10	1.49e0	3.05e0	3.13e0	3.13e0
1024	—	—	35.0	71.8	35.1	84.3	52.1	95.9
	—	—	3.40e-12	4.35e-12	4.02e-4	2.74e-5	1.05e-3	1.81e-3
2048	—	—	—	—	138.1	363.1	137.1	409.2
	—	—	—	—	3.83e-7	5.38e-7	1.85e-4	9.89e-5

EXAMPLE 3 (**Epitrochoid** ($0 \leq \alpha < 1$)**).**

$$\begin{aligned} z(t) &= e^{it} + \frac{\alpha}{2} e^{2it} \\ \theta(t) &= t. \end{aligned}$$

As $\alpha \to 1$, a cusp forms at $-\frac{1}{2}$. This non-smoothness creates some difficulties for both methods, especially for the multigrid iteration since interpolations are involved. A graph of the real part of the Szegő kernel reflects this (see Figure 5.3).

ETNA
Kent State University
etna@mcs.kent.edu

TABLE 5.3
Epitrochoid

	$\alpha = 0.9$		$\alpha = 0.95$		$\alpha = 0.99$	
n	mgw	cg	mgw	cg	mgw	cg
64	1.1	0.8	1.1	0.7	1.0	0.8
	4.69e-6	4.55e-6	5.97e-4	5.93e-4	5.32e-2	5.18e-2
128	2.9	2.0	2.8	1.9	3.4	3.3
	1.70e-9	3.59e-9	2.79e-6	2.67e-6	6.19e-3	6.14e-3
256	9.8	8.2	9.4	8.2	11.6	8.0
	7.44e-15	2.66e-15	1.32e-9	1.23e-9	3.83e-4	3.87e-4
512	—	—	36.8	34.0	36.8	37.9
	—	—	3.15e-14	1.19e-13	1.06e-6	9.74e-7
1024	—	—	—	—	215.7	196.4
	—	—	—	—	6.20e-9	6.20e-9
2048	—	—	—	—	594.6	781.9
	—	—	—	—	4.61e-13	3.56e-13

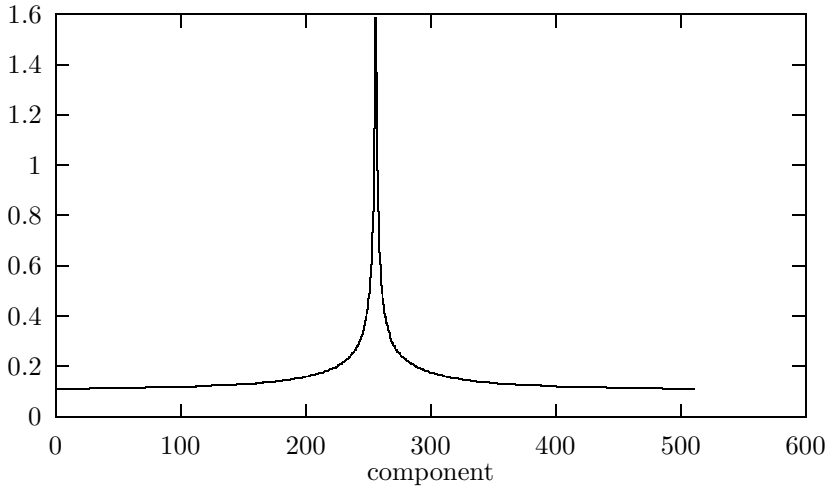

FIG. 5.3. *Real part of the Szegő kernel fo the epitrochoid,* $\alpha = 0.99$.

ETNA
Kent State University
etna@mcs.kent.edu

TABLE 5.4
Oval of Cassini

	$\alpha = 0.99$		$\alpha = 0.999$		$\alpha = 0.9999$	
n	mgw	cg	mgw	cg	mgw	cg
128	1.0	0.8	0.9	0.8	1.1	0.9
	4.87e-6	1.89e-6	6.89e-3	6.68e-3	3.25e-1	3.33e-1
256	2.8	2.5	2.2	2.2	2.3	2.3
	7.13e-11	1.57e-11	9.03e-5	8.52e-5	3.50e-2	3.52e-2
512	9.3	10.1	7.3	8.1	7.2	8.1
	2.38e-14	2.38e-14	1.71e-7	7.23e-8	1.96e-3	1.98e-3
1024	—	—	28.3	38.2	28.3	30.2
	—	—	6.51e-11	2.31e-12	8.67e-6	1.09e-5
2048	—	—	150.3	182.3	112.5	148.8
	—	—	1.67e-13	1.67e-13	3.56e-9	4.19e-9
4096	—	—	—	—	451.1	721.1
	—	—	—	—	1.67e-12	1.67e-12

EXAMPLE 4 (**Oval of Cassini ($0 \le \alpha < 1$)).**

$$\begin{aligned} |z-\alpha|\,|z+\alpha| &= 1, \\ z(t) &= \left(\alpha^2 \cos 2t + \sqrt{1-\alpha^4 \sin^2 2t}\right)^{\frac{1}{2}} e^{it}, \\ \theta(t) &= t - \frac{1}{2} arg(w(t)), \end{aligned}$$

where

$$w(t) = \sqrt{1-\alpha^4 \sin^2 2t} + i\alpha^2 \sin 2t.$$

This smooth corpuscle-shaped domain is quickly solved by both methods.

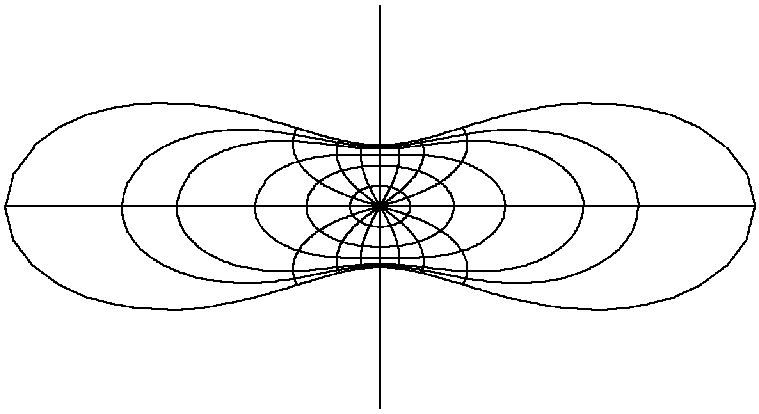

FIG. 5.4. *Oval of Cassini, $\alpha = 0.95$*

EXAMPLE 5 (**Unit square).**

$$\cos(\theta(t)) = dn(Ky),$$

ETNA
Kent State University
etna@mcs.kent.edu

TABLE 5.5
Unit square

n	mgw	cg
256	1.1	0.9
	7.51e-4	7.38e-4
512	3.7	2.3
	4.01e-4	4.06e-4
1024	13.7	8.2
	1.59e-4	1.61e-4
2048	54.1	34.5
	6.00e-5	6.09e-5

where dn denotes the Jacobian elliptic function. This boundary is only continuous, and the tangents at the corners are not even defined. We define these values as in [12]: these tangents point in the directions of the sums of their adjacent sides. Hence, we can expect some problems in the multigrid cycle (see Table 5.5).

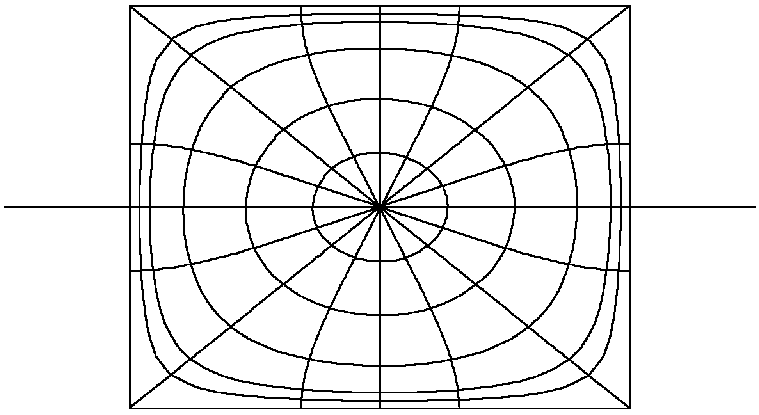

FIG. 5.5. *Unit square*

EXAMPLE 6 (**Clover leaf).** There is a cusp also in this domain. Hence, we can expect the multigrid scheme to fare worse than the conjugate gradient scheme, as confirmed in Table 5.6. Figure 5.6 reflects some of the problems in the multigrid iteration.

ETNA
Kent State University
etna@mcs.kent.edu

TABLE 5.6
Clover leaf

n	mgw	cg
256	1.0	0.8
512	3.6	2.2
1024	16.3	8.2
2048	73.4	30.4

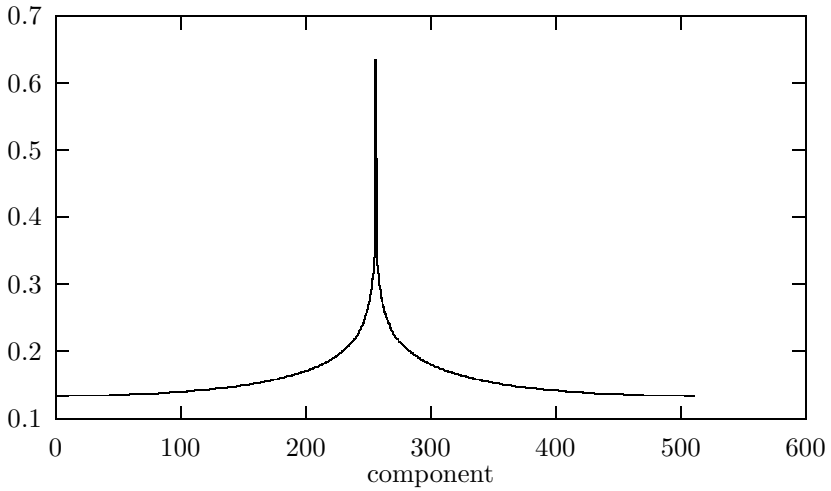

FIG. 5.6. *Real part of the Szegő kernel for the clover leaf*

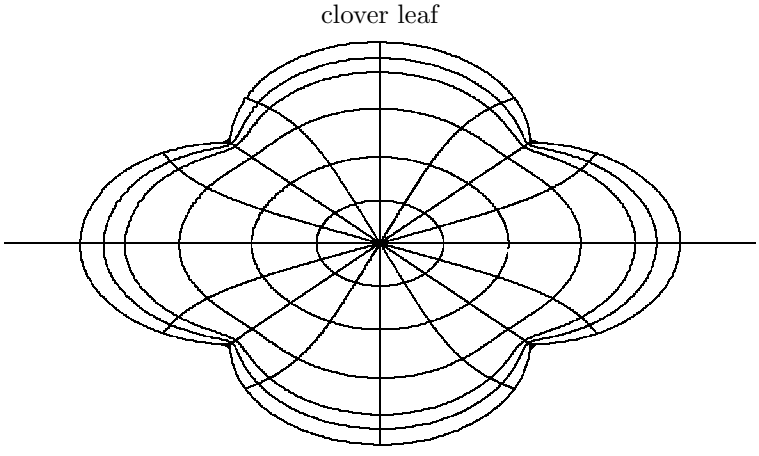

FIG. 5.7. *Clover leaf*

ETNA
Kent State University
etna@mcs.kent.edu

6. Conclusions. The numerical examples illustrate the major advantage and disadvantage of the multigrid w-cycle. For reasonably smooth regions, the w-cycle can be substantially better than the conjugate gradient method. For example, for smooth but very elongated regions, when a large number of discretization points is required on the boundary, the w-cycle can be expected to outperform the conjugate gradient approach substantially (see the results in Tables 5.2 and 5.3). However, once the boundary contains some sharp changes, the conjugate gradient iteration appears to be better. This may be expected because the norm of the two-grid matrix, and hence the multigrid iteration matrix, depends on the quadrature error.

REFERENCES

[1] M. P. Anselone, *Collectively Compact Operator Approximation Theory And Applications to Integral Equations*, Prentice-Hall, New Jersey, 1971.
[2] J.-P. Berrut and M. R. Trummer, *Equivalence of Nyström's method and Fourier methods for numerical solution of Fredholm integral equations*, Math. Comp., 48 (1987), pp. 617–623.
[3] P. Concus and G. H. Golub, *A generalized conjugate gradient method for non-symmetric systems of equations*, in Lecture Notes in Economics and Mathematical Systems, Volume 134, R. Glowinski and J.L. Lions, eds., Springer-Verlag, Berlin, 1976.
[4] D. Gaier, *Konstruktive Methoden der Konformen Abbildung*, Springer Verlag, Heidelberg, 1964.
[5] M. H. Gutknecht, *Numerical conformal mapping methods based on function conjugation*, J. Comp. Appl. Math., 14 (1986), pp. 31–77.
[6] W. Hackbusch, *Multi-Grid Methods and Applications*, Springer Verlag, Berlin, 1985.
[7] W. Hackbusch and A. Reusken, *On global convergence for nonlinear problems*, in Notes on Numerical Fluid Mechanics, Volume 23, W. Hackbusch, ed., 105-113, Fried. Vieweg, 1988.
[8] P. Henrici, *Applied and Computational Complex Analysis*, Vol. 3, John Wiley, New York, 1986.
[9] N. Kerzman and E. M. Stein, *The Cauchy kernel, the Szegő kernel, and the Riemann mapping function*, Math. Ann., 236 (1978), pp. 85–93.
[10] N. Kerzman, and M. R. Trummer, *Numerical conformal mapping via the Szegő kernel*, J. Comp. Appl. Math., 14 (1986), pp. 111–123.
[11] L. N. Trefethen, ed., *Numerical Conformal Mapping*, North-Holland, Amsterdam, 1986.
[12] M. R. Trummer, *An efficient implementation of a conformal mapping method based on the Szegő kernel*, SIAM J. Numer. Anal., 23 (1986), pp. 853–872.
[13] S. Warschawski, *On the differentiability at the boundary in conformal mapping*, Proc. Amer. Math. Soc., 12 (1961), pp. 614–620.
[14] O. Widlund, *A Lanczos method for a class of nonsymmetric systems of linear equations*, SIAM J. Numer. Anal., 15 (1978), pp. 801–812.